Chemical Isomerism as a Key to Explore Free-Energy Landscapes in Disordered Matter

C. Talón,[1] F. J. Bermejo,[2,3] C. Cabrillo,[2] G. J. Cuello,[4] M. A. González,[4] J. W. Richardson, Jr.,[5] A. Criado,[6] M. A. Ramos,[1] S. Vieira,[1] F. L. Cumbrera,[7] and L. M. González[7]

[1]*Departamento Física Materia Condensada, C-III, Universidad Autónoma de Madrid, E-28049 Cantoblanco, Spain*
[2]*Departamento Electricidad y Electrónica, Facultad de Ciencias UPV/EHU, P.O. Box 644, E-48080 Leioa, Spain*
[3]*Consejo Superior de Investigaciones Científicas, Serrano 123, E-28006 Madrid, Spain*
[4]*Institut Laue Langevin, B.P. 156, F-38042 Grenoble Cedex, France*
[5]*IPNS Division, Argonne National Laboratory, Argonne, Illinois 60439*
[6]*Departamento Física Materia Condensada, Fac. Ciencias, P.O. Box 1065, E-41080 Seville, Spain*
[7]*Departamento Física, Facultad de Ciencias, Universidad de Extremadura, E-06071 Badajoz, Spain*
(Received 28 September 2001; published 1 March 2002)

The effects of a minor chemical modification on the microscopic structure of a material in its glass and crystal phases are investigated by the concurrent use of neutron diffraction and computer simulation. Significant changes in short-, intermediate-, and long-range order are found, resulting from the change in molecular structure. These differences are explainable by a shift in the balance between directional and excluded-volume interactions.

DOI: 10.1103/PhysRevLett.88.115506 PACS numbers: 61.43.Fs, 61.12.–q

The nature of intermediate-range-order (IRO) in amorphous matter, that is the existence of spatial regularities at distances beyond those separating nearest neighbors, remains to be fully understood. Within a glass (or liquid), structural arrangements at short scales result from chemical and topological details of its constituent particles and in fact, significant progress has been achieved in our understanding of atomic arrangements in materials such as chalcogenide [1], oxide [2], or molecular glasses [3]. However, the mechanisms responsible for ordering at distances which are several times that of a characteristic unit forming the glass await clarification. Here we report on how minor chemical details such as a change in the position of a functional group within the same structural unit leads to significant changes in structure at scales well beyond those involved in short-range packing. More specifically, we have conducted neutron diffraction (ND) studies on the glass and crystal structures of the two isomers of fully deuterated propyl alcohol ($CD_3CD_2CD_2OD$ and $CD_3CDODCD_3$ referred to as 1-Pr and 2-Pr hereafter) which differ by the location of the OD group. Such an isomeric change rather than altering properties such as van der Waals volumes (124.8 and 127.7 Å^3, respectively) and electric dipole moments (about 1.66 debye) to any significant extent, leads to a change in the overall molecular "shape." The latter translates into rather different macroscopic properties such as the crystal melting points (T_m = 148 and 185 K, for 1-Pr and 2-Pr, respectively), glass-transition temperatures (T_g = 98 and 115 K), and liquid densities which differ by some 2% [4] at room temperature. Our first measurements of the $S(Q)$ static structure factors of both glasses and crystals were performed using the D4c diffractometer at the ILL (Grenoble). Crystal structure determination was achieved using the GPPD powder diffractometer at IPNS (Argonne). Although studies mostly dealing with the liquid have appeared [5], up to the authors' knowledge the crystal and glass structures of 1-Pr and 2-Pr are not known. The samples were prepared *in situ* starting from a deep quench into liquid nitrogen of room-temperature liquids and subsequent placement into a precooled cryostat. Data treatment and analysis followed standard routes for correction of sample normalization [6]. While measurement of the glass structure factors was straightforward, those for the crystals were complicated by the disparate crystallization kinetics of both isomers. As noticed previously [7], 2-Pr crystallizes spontaneously at temperatures somewhat below T_m (achieved here at 130 K) while complete crystallization of 1-Pr requires annealing over several hours at temperatures within a narrow range about 135 K. The $S(Q)$'s are shown in Fig. 1(a) and the resulting $D(r)$ total static pair correlation functions are given in Fig. 2(a). Most of the diffuse patterns in $S(Q)$'s for momentum transfers above $Q \sim 6$ Å^{-1} are attributable to details pertaining to the molecular form factors. Such correlations are suitably taken care of by subtracting from $S(Q)$ an intramolecular contribution $f_1(Q)$ [8],

$$f_1(Q) = 2 \sum_{i=1}^{M=12} \sum_{j=i+1}^{M} b_i b_j \frac{\sin(Qd_{ij})}{Qd_{ij}} \exp(-\gamma_{ij} Q^2/2), \quad (1)$$

where b_i stands for coherent scattering lengths of the ith nuclei. The sum runs over $i-j$ atomic pairs which are separated by equilibrium distances d_{ij} and the γ_{ij} are the mean-square amplitudes of atomic vibrations. The intermolecular structure factors $D_m(Q) = S(Q) - f_1(Q)$ resulting after fits to the large-Q part of $S(Q)$ of $f_1(Q)$'s estimated from molecular force-field models contain information about orientational and center-of-mass correlations and are shown in Fig. 1(b). A first remark concerns the close match between the positions Q_p of the

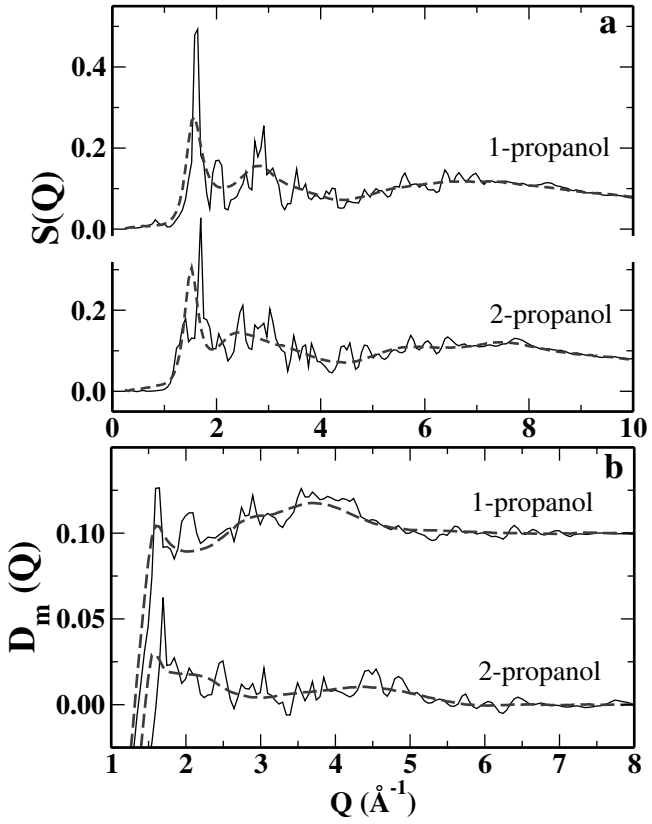

FIG. 1. (a) Static structure factors as measured on the D4 diffractometer and (b) the $D_{\mathrm{m}}(Q)$ intermolecular static structure functions derived after subtracting a $f_1(Q)$ molecular form factor. Solid line: crystals; dashed line: glasses.

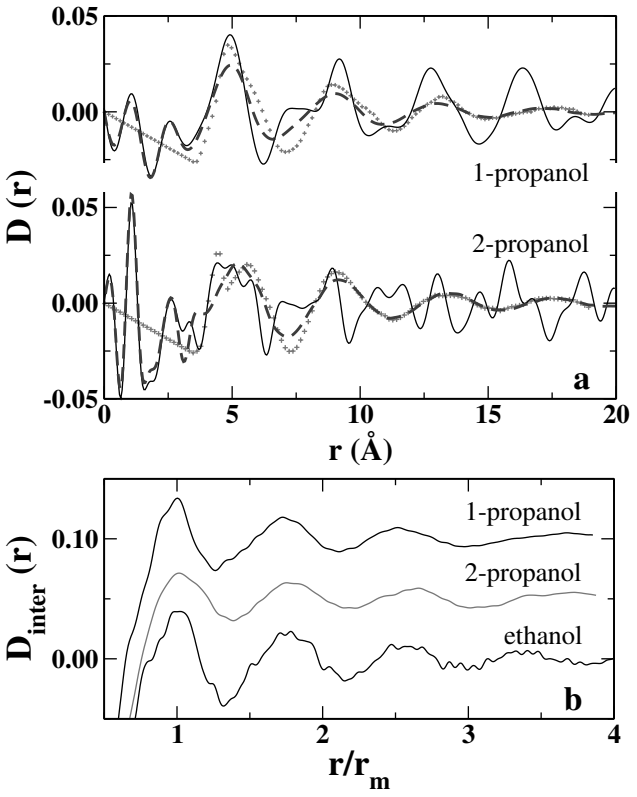

FIG. 2. (a) Total pair static correlation functions $D(r)$ as derived from experiment [solid line: crystals; dashed line: glasses; crosses: $D_{\mathrm{COM}}(r)$ as derived from computer simulations] and (b) the intermolecular pair correlation functions versus the scaled variable r/r_{m} for the glassy phases (see text).

first sharp diffraction peaks of $S(Q)$ (FSDP's) for both glasses which appear at 1.56 and 1.52 Å^{-1} and the period of the broad oscillations in the respective $D(r)$'s which come out to be $2\pi/Q_p = 4.03$ and 4.13 Å, respectively. This provides direct evidence linking the FSDP with the presence of IRO as manifested by long-period oscillations in $D(r)$ which persist up to $r \leq 20$ Å involving 4th and 5th neighbors. Since 1-Pr is significantly denser than 2-Pr, our data suggest to relate the position of the FSDP for molecular materials to the role played by the $S_{\mathrm{COM}}(Q)$ structure factor for molecular centers of mass (COM) [8] in treatments derived from liquid-state theories. To ascertain such a hypothesis, the $S_{\mathrm{COM}}(Q)$ has been evaluated for both glasses by means of computer molecular dynamics using transferable interaction potentials following steps analogous to those taken for other alcohols [9]. The results displaying $D_{\mathrm{COM}}(r)$ that is the transform into real space of $S_{\mathrm{COM}}(Q)$ are also displayed in Fig. 2(a). There one finds a fair agreement between the features exhibited by $D_{\mathrm{COM}}(r)$ and those of $D(r)$ for distances above $\approx$5 Å. Particular attention merits the presence of a double peak in the first oscillation of $D_{\mathrm{COM}}(r)$ for 2-Pr which is partially borne out by shoulders visible in the leading and trailing edges of the first $D(r)$ broad oscillation. These findings thus give support to the assignment of IRO as dominantly due to center-of-mass correlations. The $D_{\mathrm{m}}(Q)$ intermolecular structure factors displayed in Fig. 1(b) show how close the positions are of the first peaks of glassy and crystalline 1-Pr as well as a clear offset for 2-Pr, which according to what has just been discussed should be attributable to a difference in density as confirmed below. The broad diffuse background seen in the glasses for 2 Å$^{-1} \leq Q \leq 6$ Å^{-1} could be ascribed to short-ranged orientational molecular correlations as found for related materials [10]. To verify this, recourse is again made to simulation results. Several quantities which serve to quantify orientational correlations have been calculated. From within those Fig. 3 shows the orientational correlation function $\langle P_l(\cos\theta)\rangle$ where P_l stands for a Legendre polynomial and θ is an angle between molecule-fixed reference vectors which in our case are made to coincide with the direction of the O—D bonds. The result vividly shows how orientational ordering is enhanced in 2-Pr with respect to 1-Pr (i.e., larger absolute values) for distances up to $\approx$5 Å whereas that for 1-Pr covers a somewhat larger extent. In both cases these correlations vanish for $r > 6$–7 Å. The crystal $D_{\mathrm{m}}(Q)$'s appear as a pattern of Bragg peaks superimposed to diffuse patterns akin to those of the glass. We attribute such similitude to the relatively close short-range structures of glass and

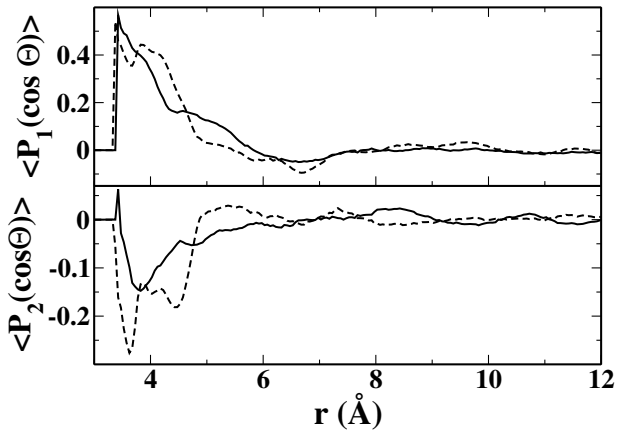

FIG. 3. Orientational correlation function $\langle P_l(\cos\theta)\rangle$ for 1-propanol (continuous line) and 2-propanol (dashed line). The figure shows the first (upper box) and second (lower box) Legendre polynomials.

crystal since at such distances structural correlations are governed by fine details of the orientation-dependent intermolecular forces (i.e., electrostatic and van der Waals, vdW) which will ultimately drive the glasses towards the fully ordered states. The data at hand thus show that for distances corresponding to first neighbors ordering is enhanced in 2-Pr. This gives us a clue about the origin of its splitted first peak in $D_{\mathrm{COM}}(r)$. In fact, detailed analysis of partial pair distribution functions derived from the simulations shows that 2-Pr has a first coordination shell ($r \leq 4.9$ Å) with most molecules participating in hydrogen bonds while bonding at larger distances becomes far less pronounced than in 1-Pr. In contrast, 1-Pr shows a more extended ordering pattern of both orientational and positional (COM) nature which may well explain the difference in macroscopic densities (0.95 and 0.90 $\mathrm{g\,cm^{-3}}$ for $T = 100$ K). Such structural change is rationalized as resulting from a shift in the balance between electrostatic and vdW forces induced by the isomeric change which changes the molecular "shape" from globular (2-Pr) to elongated (1-Pr) leaving basically unaffected the strength of the electrostatic interactions.

To check whether there are some common features in the IRO of these glass-forming materials once the difference in molecular "sizes" and "shapes" is accounted for, we now compare the Fourier transforms of $D_{\mathrm{m}}(Q)$ which give the intermolecular radial distributions versus the dimensionless variable r/r_{m}. Here r_{m} stands for an effective molecular diameter and as a measure of it we take the position of the first intermolecular peak in $D(r)$ (5.19, 5.16, and 4.68 Å for 1-Pr, 2-Pr, and ethanol [10], respectively). Such a scaled $D(r)$'s versus r/r_{m} shown in Fig. 2(b) for the three materials are now fully in phase. In other words IRO, at least in these materials, can be understood in terms of packing of equivalent sphericlike entities defined by a characteristic parameter r_{m} and extends up to distances 3–4 times longer than correlations of orientational origin.

Let us now compare the glass and crystal structures as measured by $D(r)$'s. From Fig. 2(a) one sees that while the oscillations of glass and crystal in 1-Pr show a clear phase relationship extending beyond first neighbors, those for 2-Pr follow a rather disparate pattern. To understand such distinct behaviors the crystal structures of both isomers have been determined from high-resolution powder diffraction patterns some of which are shown in Fig. 4. Indexing of such complex patterns required extreme care and labor. To do this the peak positions are first determined and powder indexing is subsequently performed [11]. The relevant structural parameters defining the unit cells of the two materials are given in Table I. From the unit cell diagrams shown in Fig. 4 together with structure data one sees that the a lattice constant for 1-Pr is roughly one and a half that for 2-Pr, which makes the number of molecules per unit cell, Z, to be 6 and 4, respectively. The space group $P\bar{1}$ for 2-Pr with $Z = 4$ indicates that the asymmetric unit consists of two independent molecules. Such unit for 1-Pr is constituted by two independent molecules located at the general Wyckoff positions $4f$ $\{(x, y, z), (-x, y + 1/2, -z), (-x, -y, -z), (x, -y + 1/2, z)\}$ and the special position $2e$ $\{(x, 1/4, z), (-x, 3/4, -z)\}$, respectively. Moreover, the $P2_1/m$ symmetry imposes that such a molecule must have an m mirror symmetry plane, that is the crystal is composed of molecules having the C-C-C-O-D skeleton within a plane. In contrast, the structure of 2-Pr corresponds to a lower symmetry lattice, a somewhat counterintuitive finding, account made of the more globular molecular shape of this isomer.

Using the crystallographic information as a constraint we have carried out a series of crystal energy minimizations using for that purpose the Cerius system. The minimum-energy structures are found to be formed by hydrogen-bonded (HB) chains along the crystal c axis with two HB per molecule. 1-Pr fits three chains within

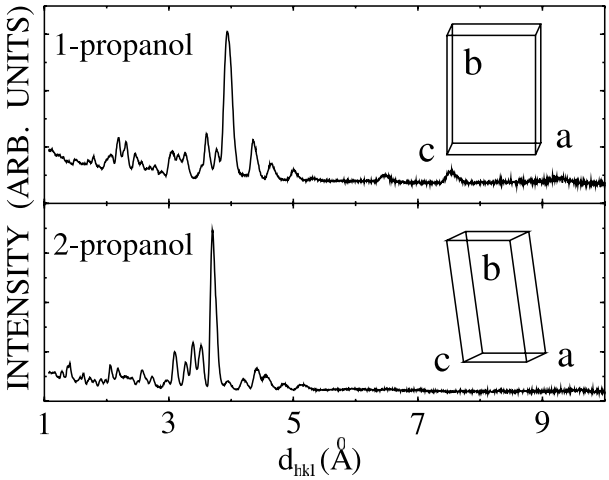

FIG. 4. Powder diffraction patterns as measured on GPPD. The insets show schematic diagrams of the two unit cells.

TABLE I. Crystal lattice parameters. The results correspond to indexing of 20 Bragg reflections and the relevant figures of merit are the $I20$ and $M20$ statistics alongside the standard deviation σ.

	Structure	Space group	a	b	c	α	β	γ	σ	I20	M20	V (Å^3)	ρ(g cm^{-3})	Z
1-propanol	Monoclinic	$P2_1/m$	9.326	12.951	5.039	⋯	96.38°	⋯	1.98×10^{-3}	20	24.0	604.91	0.99	6
2-propanol	Triclinic	$P\bar{1}$	6.612	12.891	5.653	96.58°	110.44°	97.85°	4.59×10^{-3}	20	12.6	440.43	0.91	4

the cell whereas 2-Pr just accommodates two, which explains the significantly less dense-packed structure of the latter. The calculation also predicts that crystalline 2-Pr is more stable than 1-Pr (by some 12.5 kJ mol^{-1}), a result qualitatively borne out by the difference of 37 K in melting temperatures as well as by experimental entalpies of fusion ΔH_f [7] of 5.4 kJ mol^{-1} and 6.4 kJ mol^{-1}, for 1-Pr and 2-Pr, respectively. This difference in stability explains their disparate crystallization kinetics and indeed, evaluation of the nucleation rates of critical clusters within the supercooled liquid (SCL) now made possible by data at hand by means of classical nucleation theory [12,13] shows that formation of critical clusters in 2-Pr is favored some 50 times with respect to 1-Pr. These distinct behaviors unveil large differences between the potential energy surfaces of both isomers since the formation of crystallites within a melt involves an exhaustive exploration of the free-energy landscapes (FEL). From the very concept of energy landscape [14], one expects that particles forming the SCL will mainly stay within the environment of energy minima which are not too far above the global minimum defined by the crystal configuration. Experimentally, access to some details pertaining to molecular configurations which determine the incipient clusters can be provided from information on the temperature dependence of the nucleation rate versus the chemical potentials $\Delta\mu \approx \Delta H_f(T_m - T)/T_m$ along the lines suggested in Refs. [15]. In addition, some gross features of the FEL are also amenable to experiment such as the time lags observed for nucleation and growth which are highly sensitive to details concerning the local viscosity as recently emphasized [16]. In summary, our findings exemplify how a shift in the balance between highly directional (electrostatic) and vdW interactions induced by a small change in molecular topology gives rise to a whole set of differences in structure and thermodynamics. Geometric arrangements involving nearest neighbors are found to be governed by the gross features of the interaction potential. However, contrary to oversimple assumptions our results show that changes in ordering patterns induced by the isomeric effect are far from trivial as illustrated by the enhanced short-range ordering exhibited by the material having the smaller macroscopic density. For larger distances, IRO in these materials is finally understood as a purely geometric effect, accountable in terms of packing of effectively spherical entities.

Work supported in part by Grants No. PB98-0673-C02-01 from DGICYT (Spain), Project No. BFM2000-0035-C02-01 from MCyT (Spain), and by the U.S. Department of Energy, Division of Materials Sciences, Office of Basic Energy Sciences, under Contract No. W-31-109-ENG-38.

[1] I. Petri *et al.,* Phys. Rev. Lett. **84**, 2413 (2000); D. L. Price, M. L. Saboungi, and A. C. Barnes, Phys. Rev. Lett. **81**, 3207 (1998).

[2] K. Suzuya *et al.,* J. Non-Cryst. Solids **232–234**, 650 (1998).

[3] R. Fayos *et al.,* Phys. Rev. Lett. **77**, 3823 (1996).

[4] R. C. Wilhoit and B. J. Zwolinski, J. Phys. Chem. Ref. Data **2**, Supp. 1 (1973).

[5] P. Zetterström *et al.,* Mol. Phys. **81**, 1187 (1994); B. Schiener and R. Böhmer, J. Non-Cryst. Solids **182**, 180 (1995); S. Takahara *et al.,* J. Non-Cryst. Solids **171**, 259 (1994); G. Matsui *et al.,* in *Slow Dynamics in Complex Systems,* AIP Conf. Proc. No. 469 (AIP, New York, 1999), p. 525.

[6] A. K. Soper and P. A. Egelstaff, Nucl. Instrum. Methods **178**, 4125 (1980).

[7] C. Talón *et al.,* J. Non-Cryst. Solids **287**, 226 (2001).

[8] S. C. Moss and D. L. Price, in *Physics of Disordered Materials,* edited by D. Adler *et al.* (Plenum, New York, 1985), p. 77; S. R. Elliott, Phys. Rev. Lett. **67**, 711 (1991); P. A. Egelstaff, D. I. Page, and J. G. Powles, Mol. Phys. **20**, 881 (1971).

[9] M. A. González (unpublished). For details concerning simulations on related materials, see M. A. González *et al.,* Phys. Rev. B **61**, 6654 (2000); Phys. Rev. E **61**, 3884 (2000).

[10] F. J. Bermejo *et al.,* Phys. Rev. B **56**, 11 536 (1997).

[11] The GUFI and Crysfire systems were used for peak assignment and indexation, respectively. R. Shirley, *The CRYSFIRE System for Automatic Powder Indexing: User's Manual* (The Lattice Press, Guildford, GU2 5NL, England, 1999).

[12] I. Gutzow and J. Schmelzer, *The Vitreous State* (Springer, Berlin, 1995), p. 246. The evaluation was carried out using Vogel-Tamman-Fulcher equations for the viscosity term using for the purpose recent dielectric data, M. Jiménez-Ruiz *et al.,* J. Chem. Phys. (to be published).

[13] K. F. Kelton, *Crystal Nucleation in Liquids and Glasses,* Solid State Physics (Academic Press, Boston, 1991), Vol. 45, p. 75.

[14] M. Goldstein, J. Chem. Phys. **51**, 3728 (1969); M. Schulz, Phys. Rev. B **57**, 11 319 (1998).

[15] D. W. Oxtoby and D. J. Kashchev, J. Chem. Phys. **100**, 7665 (1994); I. Gutzow, D. Kaschiev, and I. Avramov, J. Non-Cryst. Solids **73**, 477 (1985).

[16] D. J. Lacks, Phys. Rev. Lett. **87**, 225502 (2001).